# Adaptive control of a wave energy converter simulated in a numerical wave tank

Josh Davidson, Romain Genest and John V. Ringwood
Center of Ocean Energy Research,
National University of Ireland Maynooth
*E-mail: josh.davidson@nuim.ie

***Abstract*—Energy maximising controllers (EMCs), for wave energy converters (WECs), based on linear models are attractive in terms of simplicity and computation. However, such (Cummins equation) models are normally built around the still water level as an equilibrium point and assume small movement, leading to poor model validity for realistic WEC motions, especially for the large amplitude motions obtained by a well controlled WEC. The method proposed here is to use an adaptive algorithm to estimate the control model in realtime, whereby system identification techniques are employed to identify a linear model that is most representative of the actual controlled WEC behaviour. Using exponential forgetting, the linear model can be continuously adapted to remain representative in changing operational conditions. To that end, this paper presents a novel adaptive controller based on a receding horizon pseudospectral formulation.**

**The paper also demonstrates the implementation of the adaptive controller inside a computational fluid dynamics (CFD) based numerical wave tank (NWT) simulation. The adaptive controller will create the best linear model, representative of the conditions encountered in the fully nonlinear hydrodynamic CFD simulation. Using CFD presents a method to evaluate the adaptive controller within a realistic simulation environment, allowing the convergence and adaptive properties of the present control scheme to be tested.**

**A test case, considering a heaving point absorber, is presented and the adaptive controller is shown to perform well in irregular sea states, absorbing more power than its non-adaptive counterpart. The optimal trajectory calculated by the adaptive model is seen to have a smaller motion and power take-off (PTO) forces, compared to those calculated by the non-adaptive linear control model, due to the increased amount of hydrodynamic resistance estimated by the adaptive model, as identified from the nonlinear viscous CFD simulation.**

***Index Terms*—Adaptive Control, Hydrodynamic Modelling, Wave Energy Conversion, Numerical Wave Tank, OpenFOAM®**

## I. Introduction

The design of EMCs for WECs is challenging, for example:

1) WECs are correctly described by complex nonlinear equations, which are difficult to estimate
2) The models which describe WECs vary considerably in structure across different WEC types
3) The resonant behaviour of controlled WECs challenges small-signal linearisation around the equilibrium

Typically [1]–[5], a linear WEC model is determined based on Cummins equation [6], with the nonparametric hydrodynamic parameters determined using boundary-element computational tools, such as WAMIT or Nemoh. Such models assume small movement around an equilibrium point, corresponding to still water conditions. However, this assumption is challenged, since the ideal WEC behaviour is characterised by significant motion, especially when driven into resonance with the incident waves by the EMC [8], [46]. Furthermore, WEC hydrodynamics are typically characterised by nonlinearities, including viscous damping effects and nonlinear Froude-Krylov forces, where the nature and comparative extent of these nonlinearities vary considerably from device to device [9].

While some nonlinear WEC models have been incorporated into model-based WEC controllers (for example, see [10]–[12]), nonlinear control solutions are not without their problems. Although a nonlinear model structure is more likely to be a better representation of the true WEC dynamics, the control solution is often difficult, including the required solution of a nonconvex optimisation problem [11], [12].

The computational simplicity of WEC controllers based on linear models remains attractive and some progress has been made towards the determination of linear *representative* models which, although not explicitly taking nonlinear dynamic structures into account, attempt to articulate the best linear approximation to the device behaviour under realistic conditions. For example, in [13], representative linear models are determined from device behaviour measured in a CFD NWT. One important conclusion of the study in [13] is that the optimal linear parameters are sensitive to the magnitude of the WEC oscillations.

### A. Adaptive control

Considering the desirability of WEC controllers based on linear models, yet the need to capture nonlinear WEC behaviour under controlled conditions, this paper proposes an adaptive controller, which tunes the parameters of a linear WEC model, based on measured WEC responses. A receding-horizon pseudospectral optimal controller uses this linear model to determine the optimal velocity trajectory which observes the WEC physical constraints, and a lower-level backstepping controller implements the velocity-following control loop [14]. The adaptive WEC model utilised by the controller is initialised with parameters determined from a boundary-element solver (Nemoh) and the model parameters are recursively adapted using a recursive least squares (RLS) algorithm. The parameter updating enables both initial model tuning, as

  

well as continual model adaptation, to ensure relevance to any resulting changes in the dynamic WEC behaviour due to:

- Changing sea states
- Varying mooring dynamics due to slow drift motions of the WEC and changing tidal elevation [15]
- Marine growth on the WEC
- Green water on the WEC, or water leakage into the WEC
- Non-critical subsystem failure [16]

The ability of the control model to adapt in response to such changes, and remain representative of the actual WEC dynamics, has the potential to increase the controller performance across the variable conditions encountered by a WEC throughout its operational lifetime.

### *B. Numerical wave tank evaluation*

A further novel contribution of this study, is the use of a CFD-based NWT as an evaluation tool for the adaptive WEC controller. The CFD simulation environment ensures the maximum fidelity in the calculation of the WEC response, capturing important nonlinear hydrodynamic effects, such as viscous damping and nonlinear Froude-Krylov forces, which have pronounced relevance for a controlled WEC [8], [46]. Additionally, the CFD NWT provides a realistic simulation model which is different from the control model, allowing the convergence and adaptive properties of the present control scheme to be tested.

The implementation of the adaptive controller in the NWT, allows the controller to operate interactively with the CFD simulation and update its internal model, using system identification techniques on measured data of its own behaviour [17]. This has evolved from earlier work, where representative linear [13] and nonlinear [18]–[21] hydrodynamic models are identified using measured responses from WEC experiments performed in CFD based NWTs. The present adaptive control case, extends this by identifying the models online within the CFD simulation.

### *C. Outline of paper*

The paper is divided into seven sections. The field of adaptive control is discussed in Section II, and the application of adaptive control towards wave energy conversion is reviewed. Section III then presents the proposed *adaptive receding horizon pseudospectral controller* (ARHPC) for WEC energy maximisation. A description is given of; the basic linear model employed, the fundamental control calculations to implement an optimal constrained control, the velcity-profile-following backstepping controller, and the adaptation algorithm.

The use of a CFD based NWT as an evaluation tool for the adaptive control of WECs is presented in Section IV, along with implementation details of the CFD NWT and the online ARHPC - NWT interaction. A test case, showcasing a preliminary evaluation of the ARHPC in the NWT, is presented in Section V. A discussion of the keypoints of the paper is given in Section VI, and conclusions are drawn in Section VII.

## II. Adaptive control of wave energy converters

An adaptive controller can modify its behaviour in response to changes in the dynamics of the system and/or in the character of the excitations. Adaptive controllers can be defined as *"a controller with adjustable parameters and a mechanism for adjusting the parameters"* [22]. Research grew in the early 1950s, motivated by design of autopilots for aircraft [23], and has continued since, including applications analogous to wave energy, such as vibration energy harvesting [24] and wave absorption in a wave tank/flume [25].

Adaptive control enables estimation of uncertain, unknown or time-varying parameters on-line using measured system signals. The requirements of the measured signals for identification of a WEC model are discussed in [26], with regard to the amplitude and frequency range that the signals must span, to provide information rich data from which the dynamical behaviour of the system can be identified. Fortunately, a controlled WEC receives persistent excitation, thus is well suited for on-line model identification during its normal operation. The estimation of parameters can be performed on a self-tuning or adaptive basis. Self-tuned parameter values converge on fixed values, whereas adaptive parameter values are continually estimated with stronger bias towards recent data.

Adaptive control has been applied to the field of wave energy. An early study is given by the authors in [27], who apply their initial work in [25] successfully to an oscillating water column WEC. The adaptive controller is based on a Kalman filter frequency tracking algorithm, that provides an on-line estimation of the "instantaneous wave frequency". The adaptive controller is shown to compare favourably with more conventional open-loop systems.

A comparison of selected adaptive control strategies for WECs, such as gain scheduling and extremum-seeking adaption, is presented in [4]. [1] discusses that optimal causal control is only a viable approach if the controller parameters adapt to changes in the sea state, showing the necessity of gain-scheduling in accordance with changes in the spectral content and propagatory direction of the sea state. Techniques can be framed in an indirect adaptive control context, in which the optimal LQG controller is continually adapted to an updated identified model based on measured output data. This is analogous to adaptive tuning techniques proposed in prior studies [28], in which control parameters are modified in response to detected changes in wave period and amplitude. The simple and effective real-time controller in [28] drives the WEC motion in phases with the wave excitation force, and ensures amplitude constraints are obeyed, by tuning one single parameter of direct physical meaning.

[29] show how the control strategy applied to point absorbers in heave, can be effectively tuned according to the changes in the incident waves. The aim is to maximize the average power extraction at each given wave, while limiting the value of the instantaneous power. [30] apply this control approach, adapting the resistive and reactive PTO

force components on a wave-to-wave basis. The reactive component, while improving average power extraction, can result in excessive over rating of the PTO. [31] shows how a convenient tradeoff between high-power extraction and viable electrical device rating can be achieved by a proper choice of the WEC control strategy. Its effectiveness in increasing the average power extraction while respecting the PTO peak power constraint, is proved by computer simulations in both regular and irregular waves.

[32] presents wave prediction and fuzzy logic control of WECs in irregular seas, where the short term resistive and reactive components of the PTO force are Fuzzy Logic based control designed according to online wave prediction. [33], [34] also employ adaptive Fuzzy Logic based control for the resistive and reactive components of the PTO force. The resistive and reactive components of the PTO force are adapted using reinforcement learning in [16], and maximum power point tracking (MPPT) in [35]. MPPT is also used in [36] to adapt the resistive component of the PTO force only.

[37] deals with uncertainties in control model parameters, by using adaptive control to improve the approximation to system parameters, such as: mass, viscous damping coefficient, hydrostatic stiffness, the radiation impulse-response and the exciting force impulse-response functions.

## III. The Adaptive Receding Horizon Pseudospectral Controller

The structure of the control algorithm can be divided into three parts, depicted in Fig. 1. The main part considers the optimal trajectory determination (under path constraints), using a receding-horizon pseudospectral control (RHPC) [14], leading to the optimisation of a quadratic problem. The second part, then determines the control force to apply on the system to follow the given reference trajectory, from the RHPC. A backstepping method is employed to realise the trajectory tracking task, due to inherent control model/CFD simulation mismatch. The third part, working in parallel, adapts the linear control model in real time, using a standard recursive least square (RLS) algorithm. The linear control model allows fast calculation of the optimal control trajectory via standard tools for the optimisation of quadratic problems.

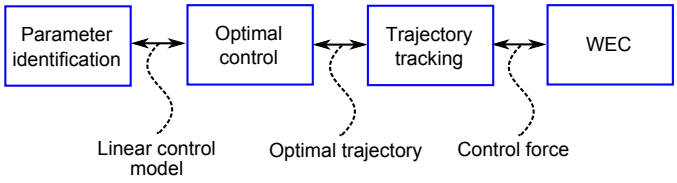


Fig. 1. Simplified diagram of the control algorithm structure

### A. Optimal control

The optimal control generates a trajectory that maximises a given cost function, while respecting path constraints over a given control horizon. In the present application, the cost function corresponds to the energy absorbed by the WEC, and path constraints are typically amplitude and/or force limitations. Several control strategies are commonly employed in order to derive the optimal trajectories that the system should follow, such as model predictive control (MPC) [38], or pseudospectral control [5]. In the present study, the optimal control algorithm is based on a RHPC [14].

*1) Receding horizon pseudospectral control:* The state and control variables are approximated by their truncated series on a given set of orthogonal functions on a fixed control horizon $I = [t, t + T_0]$, where $t$ is time and $T_0$ the control horizon over which the energy absorption is maximised.

$$\forall t \in I, f(t) \approx f^N(t) = \sum_{i=1}^{N} \tilde{f}_i \phi_i(t) = \mathbf{\Phi}(t)\tilde{\mathbf{f}} \tag{1}$$

with,

$$\tilde{f}_i = \int_I \phi_i(t) f(t) dt \tag{2}$$

Note that the function $f(t)$ in Eq. (1) could either be a control or a state variable. $f^N(t)$ is a truncated series that approximates the initial function as a finite sum of weighted basis functions, $\mathbf{\Phi}(t) = \{\phi_i(t)\}_{i=1}^N$. The vector, $\tilde{\mathbf{f}} = [\tilde{f}_1, \ldots, \tilde{f}_N]^T$, contains the projections of $f(t)$ onto the basis functions. In the present work, the basis functions chosen for the optimal control are half-range Chebyshev Fourier functions, defined in [39], and employed in a RHPC in [14].

The performance function maximised by the control algorithm corresponds to the absorbed energy over the control horizon $I$,

$$J = -\int_I v(t)u(t)dt \tag{3}$$

where $v(t)$ is the velocity of the WEC system and $u(t)$ corresponds to the control force applied to the WEC, generated by a PTO system. Replacing the state and control variable by their truncated series, we obtain the following evaluation of the cost function,

$$J \propto -\tilde{\mathbf{v}}^T \tilde{\mathbf{u}} \tag{4}$$

Since all the basis functions are orthogonal, the cost function is directly proportional to the sum of the product of the projections of the velocity $\tilde{v}_i$ and the control force $\tilde{u}_i$. This leads to a convex optimisation problem; a strength of this linear control formulation.

While maximising the cost function $J$, the control algorithm must ensure that the dynamical equations describing

the system behaviour are satisfied by the state and control variables involved in the control calculation, i.e. the position, velocity and control force projections, represented by $\tilde{\mathbf{x}}, \tilde{\mathbf{v}}$ and $\tilde{\mathbf{u}}$, respectively. The two differential equations describing the system dynamics are:

$$\frac{dx(t)}{dt} = v(t) \tag{5}$$

which links position and velocity, and

$$(m+\mu_\infty)\frac{dv(t)}{dt}+\int_0^t K_r(t-\tau)v(\tau)d\tau+S_h x(t) = F_{ex}(t)+u(t) \tag{6}$$

which is the Cummins' equation [6] derived from a linearised version of Newton's second law of motion applied to the WEC. Here, $m$ and $\mu_\infty$ are the proper mass and the infinite frequency added mass of the system, $K_r(t)$ is the kernel function involved in a convolution product with the velocity, representing a linearised version of the radiation force, $S_h$ is the hydrostatic stiffness, while $F_{ex}(t)$ is a linearised expression of the excitation force generated by unperturbed incoming waves onto the WEC's hull, at its equilibrium position.

Expressed in terms of residuals, and replacing each state and control variables by the truncated series, we obtain the following linear equations:

$$\begin{aligned} r_1(t) &= \mathbf{\Phi}(t)\left[\mathbf{D}\tilde{\mathbf{x}} - \tilde{\mathbf{v}}\right] \\ r_2(t) &= \mathbf{\Phi}(t)\left[((m+\mu_\infty)\mathbf{D}+\mathbf{R})\tilde{\mathbf{v}} + S_h\tilde{\mathbf{x}} - \tilde{\mathbf{u}}\right]\ldots \\ &\quad +F_r(t) - F_{ex}(t) \end{aligned}$$

where $\mathbf{D}$ is the differential matrix defined in [40], $\mathbf{R}$ is the radiation matrix defined in [14], corresponding to the radiation force generated by the velocity over the control horizon $I$. $F_r(t)$ is the radiation force generated by past value of the velocity affecting the control horizon. For more details on the RHPC algorithm, the reader may refer to [14] and [41].

Path constraints, such as control force or position excursion limits, can be easily taken into account by the RHPC algorithm. For example, in order to avoid any slamming phenomenon that could occur if the device comes out of the water, as can happen when applying complex-conjugate control without position constraints, the relative position of the body with respect to the actual free surface is restrained to be smaller than a given geometrical parameter $H$,

$$|\mathbf{\Phi}(t)\tilde{\mathbf{x}} - \eta(t)| \leq H \tag{7}$$

The control algorithm needs to maximise the cost function $J$, bring the residuals $r_1$ and $r_2$ to zero and ensure the satisfaction of linear inequality constraints. The optimisation problem is quadratic and is solved using the *quadprog* function in MATLAB. The optimisation problem is re-solved for every new control horizon $I$.

*2) Control model interpretation and initialisation:* The Cummins' equation used in the RHPC is expressed in terms of state and control variable projections and is evaluated at each collocation point, $t_k$, as

$$\mathbf{\Phi}(t_k)\left(\mathbf{G}\begin{bmatrix}\tilde{\mathbf{x}}\\ \tilde{\mathbf{v}}\end{bmatrix} - \tilde{\mathbf{u}}\right) = F_{ex}(t_k) - F_r(t_k) \tag{8}$$

Rewriting the matrix $\mathbf{G}$ as the combination of two submatrices $\mathbf{M}$ and $\mathbf{N}$, operating only with the projections of position and velocity, $\tilde{\mathbf{x}}$ and $\tilde{\mathbf{v}}$, respectively,

$$\mathbf{\Phi}(t_k)\left([\mathbf{M},\mathbf{N}]\begin{bmatrix}\tilde{\mathbf{x}}\\ \tilde{\mathbf{v}}\end{bmatrix} - \tilde{\mathbf{u}}\right) = F_{ex}(t_k) - F_r(t_k) \tag{9}$$

and then, by developing the linear equation of the system, we obtain:

$$\sum_i\sum_j m_{ij}\tilde{x}_i\phi_j(t_k) + \sum_i\sum_j n_{ij}\tilde{v}_i\phi_j(t_k) = F(t_k) \tag{10}$$

where $F(t) = u(t) + F_{ex}(t) - F_r(t)$ represents the sum of the control, excitation and *past velocity generated* radiation forces acting on the device. The two double sums can be seen as a projection of the position and velocity onto given kernel functions, $m$ and $n$, respectively, such that

$$\sum_i\sum_j m_{ij}\tilde{x}_i\phi_j(t) = \int_I m^N(t,\tau)x^N(\tau)d\tau \tag{11}$$

$$\sum_i\sum_j n_{ij}\tilde{v}_i\phi_j(t) = \int_I n^N(t,\tau)v^N(\tau)d\tau \tag{12}$$

where $m^N(t,\tau) = \sum_i\sum_j m_{ij}\phi_i(\tau)\phi_j(t)$ and $n^N(t,\tau) = \sum_i\sum_j n_{ij}\phi_i(\tau)\phi_j(t)$. The equation of motion is then transformed in a Fredholm integral equation of the first kind, as:

$$\int_I m^N(t,\tau)x^N(\tau)d\tau + \int_I n^N(t,\tau)v^N(\tau)d\tau = F(t) \tag{13}$$

From Cummins'equation, the initial kernel functions $m_0^N$ and $n_0^N$ can be written as follows:

$$m_0^N(t,\tau) = S_h\delta(t-\tau) \tag{14}$$

$$n_0^N(t,\tau) = (m+\mu_\infty)\dot{\delta}(t-\tau) + K_r(t-\tau) \tag{15}$$

where $\delta$ and $\dot{\delta}$ correspond, respectively, to the Dirac delta function and its first derivative. This illustrates the ability of the model formulation to represent the standard Cummins equation. The control model parameters can be initialized from Eqs. (14) and (15), using hydrodynamic parameter values, $S_h, \mu_\infty$ and $K_r(t)$, obtained from a BEM solver such as WAMIT or Nemoh.

### B. Parameter identification

The model in Eq. (8), based on the definition of the matrix $\mathbf{G}$, is updated at each $T_{RLS}$ time-step, using on a standard RLS algorithm [42]. The RLS algorithm will try to reach the best kernel functions, $m^N$ and $n^N$ from Eq. (13), to satisfy the equation of motion of the system. At a given RLS time step $p$, the linear model is updated in the following manner:

$$\begin{aligned}
\theta &= [\tilde{\mathbf{x}}^T, \tilde{\mathbf{v}}^T]^T && (16)\\
\mathbf{e}(p) &= \mathbf{d}(p) - \theta^T \mathbf{G}^T(p-1) && (17)\\
\mathbf{r}(p) &= \mathbf{P}(p-1)\theta / (\lambda + \theta^T \mathbf{P}(p-1)\theta) && (18)\\
\mathbf{P}(p) &= \lambda^{-1}\left(\mathbf{P}(p-1) - \mathbf{r}(p)\theta^T \mathbf{P}(p-1)\right) && (19)\\
\mathbf{G}(p) &= \mathbf{G}(p-1) + \mathbf{e}(p)\mathbf{r}(p) && (20)
\end{aligned}$$

where the matrix $\mathbf{P}$ is initialised as $\mathbf{P}(0) = p_0\mathbf{I}$ (where $\mathbf{I}$ represents the identity matrix). The vector $\mathbf{d}$ is the measured outputs that the linear model should emulate, which in this case is the projection of the sum of the excitation, radiation and control forces. $\lambda$ is the forgetting factor, allowing a self-tuning control ($\lambda = 1$) or an adaptive control ($0 < \lambda < 1$).

### C. Tracking trajectory

Since the simulation model is different from the control model, and generates nonlinear fluid forces, a backstepping method is employed to make the system follow the optimal trajectory determined by the RHPC. This follows the general robust hierarchical structure in [43], while backstepping employing feedback linearisation is shown to have good robustness properties in [44]. The backstepping control is based on a linear Cummins' equation type WEC model. Since the Cummins' equation is a second order partial differential equation, backstepping control involves two *error functions* $V_1(t)$ and $V_2(t)$ which need to be Lyapounov stable:

$$V_1(t) = \frac{1}{2}e_1^2(t) \tag{21}$$

where $e_1(t) = x(t) - x_{ref}(t)$ is the error between the measured WEC position, $x(t)$, and the reference trajectory, $x_{ref}(t)$, and

$$V_2(t) = V_1(t) + \frac{1}{2}e_2^2(t) \tag{22}$$

where $e_2(t) = v(t) - v_{ref}(t)$ is the error between the measured WEC velocity, $v(t)$, and the reference trajectory, $v_{ref}(t)$. Thus, by differentiating $V_2(t)$ and using Cummins' equation, the control force $F_{PTO}(t)$ is defined to achieve Lyapounov stability for $V_1(t)$ and $V_2(t)$, as

$$\begin{aligned}
F_{PTO}(t) &= -(m+\mu_\infty)(e_1(t) - \ddot{x}_d(t) + \tau_2 e_2(t)) \ldots \\
&\quad + S_h x(t) + \int_0^t K_r(t-\tau)v(\tau)d\tau - F_{ex}(t)
\end{aligned}$$

where $\tau_1$ and $\tau_2$ are constants (in $s^{-1}$) defining the rate of convergence of $V_1(t)$ and $V_2(t)$ and $\dot{x}_d(t) = v_{ref}(t) - \tau_1 e_1(t)$ is an intermediate variable related to the desired velocity. For more details on the implementation of the backstepping method, the reader may refer to [14].

## IV. Numerical wave tank simulation of the adaptive controller

A NWT provides a cost effective means of device experimentation and evaluation. Developing an economically competitive WEC requires early device optimisation using numerical tools [45]. An economically competitive WEC will likely employ an EMC, therefore, evaluating EMC performance in a NWT can prove useful.

Classically, EMC evaluation has relied on linear model simulations. However, the increased amplitude of WEC dynamics under controlled conditions challenge the validity of the small amplitude linearising assumptions of such models [8], [46]. CFD, on the other hand, has a greater range of validity when simulating large amplitude WEC motions, by considering nonlinear effects such as viscosity and time-varying wetted body surface area. Consistent with the observations in [47], the results in [13] show that increasing the amplitude of the WECs operation away from its zero amplitude equilibrium state, leads to a divergence between a linear hydrodynamic model and a CFD simulation. Specifically, the levels of hydrodynamic damping experienced by a WEC are seen to increase as the amplitude of operation increases. Therefore, evaluating an EMC with a linear model will likely result in predictions of unrealistically large WEC motions and energy capture due to an underestimation of the hydrodynamic damping on the WEC [8].

The CFD based NWT provides a fully nonlinear hydrodynamic simulation, allowing the convergence and adaptive properties of the present control scheme to be tested. The ARHPC will create the best linear control model representative of the conditions encountered in the nonlinear simulation. The identification of parametric hydrodynamic models, from input/output data obtained from CFD experiments, has been demonstrated in [17]–[21]. The present adaptive control scheme takes this system identification approach a step further, by identifying the models online within the simulation. The CFD based NWT provides an useful tool for developing the ARHPC and other adaptive EMCs.

### A. Implementation

The NWT is implemented using the open source CFD software, OpenFOAM, as detailed in [48]. This type of NWT has previously been used for evaluating the controlled operation (Proportional-Integral (PI) control [8] and latching control [7]) of a heaving sphere point absorber type WEC. A similar implementation methodology is employed here, with the addition of the OpenFOAM simulation being coupled with MATLAB, to allow calculation of the optimal control.

The adaptive controller, in this paper, is implemented using MATLAB, and therefore requires a communication pipe with the OpenFOAM simulation. This is achieved following a similar procedure described in [50], where mooring forces are calculated via a MATLAB interface and are applied to an OpenFOAM simulation of a moored WEC. In the present application, the MATLAB interface is used to calculate the PTO force via the ARHPC algorithm.

### B. Simulation structure

The global architecture of the control algorithm and its simulation environment is shown in Fig.2. The control algorithm can be decomposed into three distinct stages running with individual time-steps:

- The backstepping controller (*Green*) is contained as a routine within the NWT simulation, and updates the control force at each CFD time step $\Delta t_{CFD}$. The motion reference trajectory, providing the input to the backstepping controller, is defined by its projections onto the orthogonal set of basis functions, and thus can be easily estimated at any given instant without the need of interpolation, simplifying the connection of high-level (MATLAB) and low-level (OpenFOAM) control environments.
- The ARHPC (*Red*) computes the reference trajectory iteratively at a regular time-step, $\Delta t_{PS}$. The solution of the reference trajectory projection maximises the energy absorption, while ensuring path constraints.
- The adaptive algorithm (*Blue*) updates the linear model of the system at a regular time-step $\Delta t_{RLS}$. The updated linear model is then stored and used by the RHPC to find the reference trajectory. The choice of $\Delta t_{RLS}$ is important, in that it must be chosen short enough to allow good tracking of changes in a linear *representative* model corresponding to sea state variations, while not so short as to attempt instantaneous tracking of the nonlinearities.

The excitation force (*White*) must be estimated over the future control horizon $T_0$. Different methods are available for the excitation force prediction, and the NWT provides a tool for evaluating the sensitivity of an EMC to the error in that prediction. In the present paper, the effect of the excitation force prediction is removed, and the ARHPC is evaluated under the assumption of perfect knowledge of the incident wave series. The incident wave series is first created in an empty NWT, and the free surface elevation (FSE) measured at the location corresponding to the WEC centre of mass. The WEC is given the FSE measurements and then placed in the NWT with the same wave series simulated.

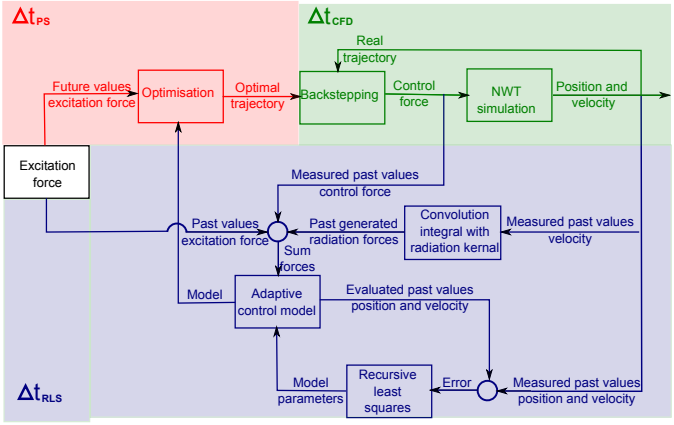


Fig. 2. Global architecture of the control algorithm and the CFD simulation

## V. Test case

An illustrative example of the ARHCP simulated in a NWT is given in this section. The test case is described in Section V-A and then the results presented in Section V-B.

### A. Description

*1) WEC:* The test case considers a relatively simple WEC: a spherical buoy, constrained to heave motion only, equipped with an ideal PTO capable of providing/extracting bidirectional power to/from the heaving buoy, see Fig.3-(a). The mass density of the WEC is half of the water density (1020kgm$^{-3}$), so that the sphere is 50% submerged at equilibrium. The non-uniform cross-sectional area of the sphere, results in nonlinear Froude-Krylov forces, for the large variations in wetted surface typically manifest under controlled conditions.

The sphere has a $0.1m$ radius and $0.61s$ natural period; representing a scaled down version of a realistic WEC, chosen to reduce the required NWT computation time. The differences in run times, for CFD simulations of model and full scale WECs, is discussed in [52]. The smaller WEC, and shorter wave lengths, require less mesh cells in the NWT spatial discretisation (shown in Fig. 3-(b)). The shorter wave period allows more wave cycles per simulation time.

*2) Tank:* The NWT has a length and width of $10m$, filled with $3m$ of water, and the WEC is located in the centre of the tank at the free surface (note a symmetry plane bisects the NWT, reducing the simulated tank width to $5m$). Waves are generated at one end of the tank, and absorbed at the other end, using the relaxation method implemented in the waves2Foam toolbox [51]. A post process view of the dynamic pressure in the NWT is Fig. 3-(c) illustrates the wave creation and absorption in the different ends of the tank.

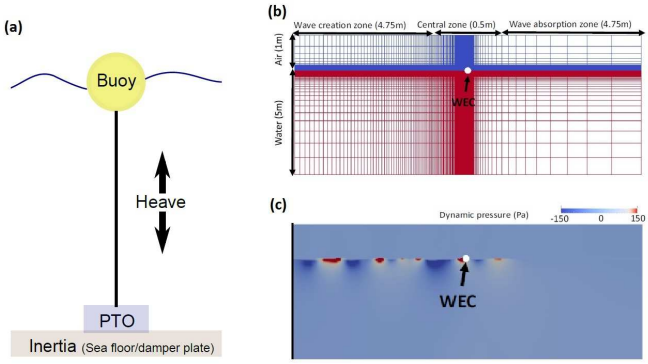


Fig. 3. (a) Schematic of the WEC (b) Cross section of the mesh, fluid volumes (water=red, air=blue) and WEC at equilibrium in the NWT (c) Post Process view of the dynamic pressure in the NWT during the OpenFOAM simulation.

*3) Input waves:* An input wave series representing a JONSWAP spectrum, consisting of 100 frequencies non-uniformly distributed between 0 and $2Hz$ with random phases, and a peak period of $1s$, is employed (see Fig. 4). Note the peak period differs from the natural period of the WEC, $0.61s$.

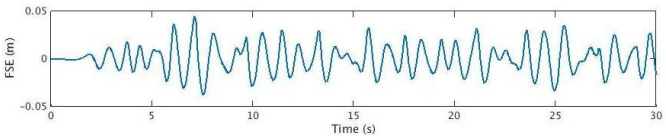


Fig. 4. Measured free surface elevation (FSE) at the centre of the tank.

*4) Tests:* Two tests are presented; *Test 1* and *Test 2*. In both tests, the input wave conditions created in Fig. 4 are used for the WEC simulation, implementing both an adaptive and a constant control model.

*Test 1* investigates the adaptation of the linear ARHPC to the nonlinear conditions in the NWT simulation. The parameter adaptation will be monitored as it evolves throughout the simulation. The ARHPC performance is measured against the same controller using constant model parameters only. The test (NWT, WEC and input wave series), is exactly the same as presented in [8], excepting the use of a proportional-integral (PI) controller in [8]. The ARHPC performance will therefore, also be compared against these PI control results.

The PI controller, shifts the WEC natural frequency by changing the system reactance with the PTO force, to resonate the WEC with the input wave spectrum. The proportional and integral to the velocity terms are tuned to achieve complex conjugate impedance matching. In this case, impedance matching is approximated, by matching the resistive term with the WEC radiation damping at the peak wave period and matching the WEC natural period with the peak wave period using the reactive term [53]. For the PI controller in [8], the integral term had a stiffness parameter value of $-197N/m$ for the reactive force component, and the proportional term had a damping parameter value of $6.22Ns/m$ for the resistive force component.

*Test 2* investigates the ability of the ARHPC to adapt to changes in the WEC physical parameters. In this test the WEC mass is increased by 10% in the CFD simulation. Increasing WEC mass may occur in reality, due to marine growth or water leakage into the WEC hull for example.

*5) Control settings:* The value for the various control parameters used by the ARHPC, and its non-adaptive counterpart, are listed in Table I.

TABLE I
CONTROL SETTING VALUES USED IN THE TEST CASE EXAMPLES.

| Parameter | Symbol | Value |
|---|---|---|
| Control horizon | $T_0$ | $2s$ |
| RLS update period | $\Delta t_{RLS}$ | $0.2s$ |
| Optimal trajectory update period | $\Delta t_{PS}$ | $1ms$ |
| RLS forgetting factor | $\lambda$ | 0.995 |
| **P** initialisation | $p_0$ | 1 |
| Number of basis functions | $N$ | 7 |
| Geometrical constraints | $H$ | $0.1m$ |

*6) Model initialisation:* Choosing seven basis functions for the RHPC controllers, leads to a linear control model, $\mathbf{G}$, comprising two $15 \times 15$ submatrices, $\mathbf{M}$ and $\mathbf{N}$. Using hydrodynamic parameters calculated from the BEM solver *Nemoh*, the parameter values for $\mathbf{M}$ and $\mathbf{N}$ are initialised using Eqs. (14) and (15), respectively, and are displayed in Fig. 5. The matrix $\mathbf{M}$ can be seen to be diagonal, with the non-zero parameters equal to the hydrostatic stiffness $S_h$. The matrix $\mathbf{N}$ contains parameters related to both velocity and acceleration dependent forces, with the upper left and lower right quadrants relating to the velocity terms, and the upper right and lower left quadrants relating to the acceleration terms.

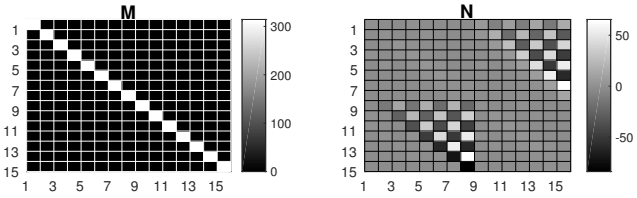


Fig. 5. Initialisation of the $M$ and $N$ matrices

*7) CFD settings:* While care is taken to ensure realistic simulations, extensive verification and validation producing quantitative measures of the error, as described in [54], is not undertaken for this preliminary demonstration of the ARHCP evaluation in the NWT. Instead a pragmatic approach, using a qualitative mesh convergence study is employed, ensuring both a grid-independent solution and a reasonable run time.

Testing of the wave creation and absorption followed procedures detailed in [55], resulting in a vertical mesh resolution of $5mm$ around the free surface. The mesh around the WEC is then examined, as depicted in Fig. 6, where $M1$ uses the base mesh with a nonuniform first cell thickness of maximum value $5mm$, and $M2$ and $M3$, use refinement layers to achieve a uniform first cell thickness of $3mm$ and $1mm$, respectively. The graph in Fig. 6, of the resulting WEC motion for the three different mesh setups, shows that the refined mesh $M2$ gives the same results as the even further refined mesh $M3$, and therefore $M2$ is used for the subsequent simulations. A total of 882,000 cells are used in the NWT. The laminar simulations use an adjustable time stepping approach, ensuring a maximum Courant number of 0.9, resulting in timesteps, $\Delta t_{CFD} = \mathcal{O}(10^{-4}s)$.

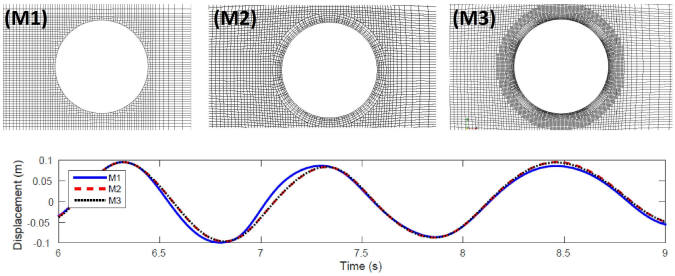


Fig. 6. Mesh convergence study.

### B. Results

*1) Test 1:* The performance of the ARHPC versus its non-adaptive counterpart is shown in Fig. 7, which plots the WEC (a) displacement, (b) PTO force and (c) energy absorption for the input wave series in Fig. 4. The adaptive algorithm is initiated after $3s$, and Fig. 7 shows that both controllers perform identically for the first $3s$. The performance of the two controllers then begin to diverge after the parameters of the adaptive control model start to be updated. The model adaptation leads to the ARHCP calculating an optimal trajectory with smaller amplitude displacement and PTO forces, yet yielding more energy than the controller with a constant control model.

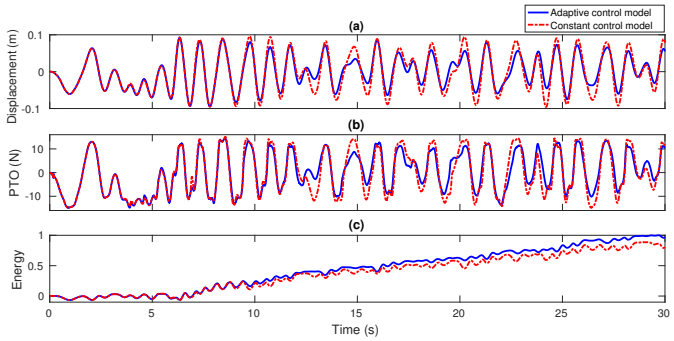


Fig. 7. Results of the adaptive RHPC versus the constant RHPC

Fig. 8 shows the total change in parameter values, for the $\mathbf{M}$ and $\mathbf{N}$ matrices, at $T = 30s$. The diagonal entries of $\mathbf{M}$, whose parameters correspond to $S_h$, are seen to change due to the adaptive algorithm. Fig. 9-(a) plots the evolution of the first three diagonal entries, showing a decrease in parameter values once the adaptation begins. A decrease in the adaptive models representation of $S_h$ makes sense physically, considering that the value of $S_h$ for the considered sphere is maximum at its equilibrium position and decreases when the sphere moves in or out of the water. The adaptive model parameters therefore update to a linear average of the reduced $S_h$ values encountered while the sphere is away from its equilibrium. Similarly, Fig. 9-(b) shows the evolution of the first three diagonal entries of the matrix $\mathbf{N}$, which correspond to pure damping forces, and in this case, the parameter values increase with the adaptation. These parameters are initialised considering linear radiation forces, but due to the additional viscous damping forces in the NWT, the adaptive model increases its linear representation of the total damping forces.

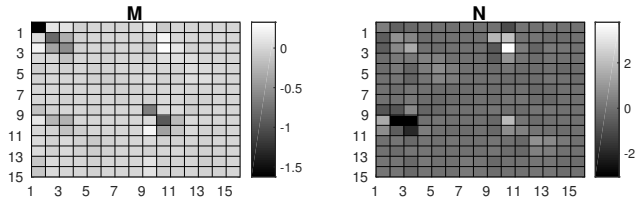


Fig. 8. Changes to parameters in the $M$ and $N$ matrices

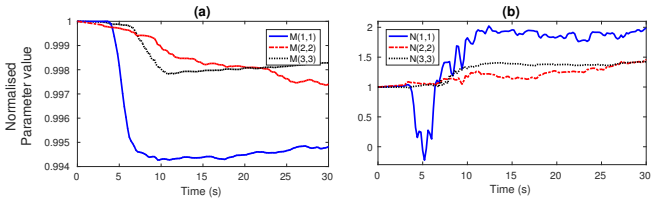


Fig. 9. Adaption of parameters over time

The ARHPC is compared against the PI controller in Fig. 10. The results show that the ARHPC absorbs about 50% more energy than the PI control over the last $20s$ of the simulation.

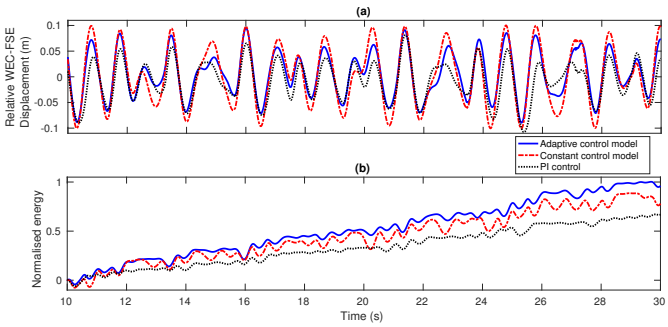


Fig. 10. Results of the adaptive controller versus the PI controller

*2) Test 2:* Similar relative performance, between the adaptive and constant controllers, were observed in this test as in *Test 1*. Also similar changes to the adaptive model parameters were observed. An interesting result concerning this test is shown in Fig. 11, comparing the results of the constant controller in *Test 1* and *Test 2*. Although the parameter values of the constant control model in *Test 2* misrepresents the WEC mass by 10%, the total energy absorbed is the same as in *Test 1*. The misrepresentation of the WEC inertia results in more reactive power being added and removed from the WEC controller each cycle, but the overall absorbed power remains the same.

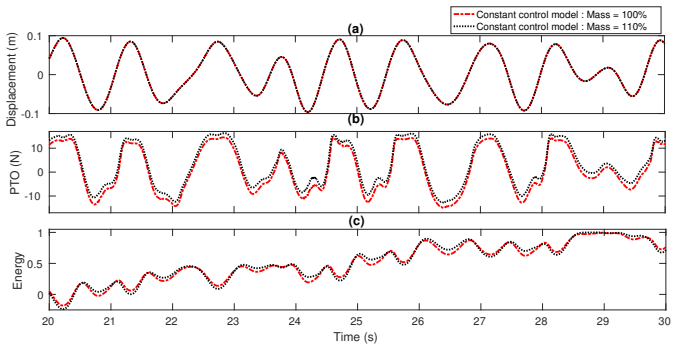


Fig. 11. Comparison of the constant controller results when the WEC mass is increased by 10% in the CFD simulation versus the *Test 1* results.

## VI. Discussion

Comparing the performance of the ARHCP and its non adaptive counterpart, the results demonstrate the improved performance of the optimal controller, when the control model accurately represents the WEC hydrodynamic resistance. When optimal PTO control is considered as an impedance matching exercise, the optimal PTO force matches the complex-conjugate of the WEC mechanical impedance, described in [53], [56]. The optimal PTO force is therefore dependent on an accurate measurement of, (1) the excitation force, and (2) the resistive term of the WEC's total mechanical impedance. The results presented in this paper have focussed on using adaptive system identification techniques to optimise the control model's estimation of (2). The linear control model representation of the resistive hydrodynamic forces, was adaptively increased by the ARHPC to account for added hydrodynamic resistance in the NWT simulation (due to viscous effects such as drag and vortex shedding). Correspondingly, the optimal trajectory calculated by the ARHPC decreased in amplitude, due to the adapted control model predicting increased amounts of energy dissipation for large velocities.

An interesting result to come from *Test 2*, is the lack of sensitivity to the control model estimate of the inertia terms. This result agrees with the findings in [56], showing the dominating influence of the WEC mechanical resistance on the optimal control impedance, compared with the mechanical reactance terms. The results in Fig. 11 show that incorrect control model knowledge of the true WEC mass, results in a temporary loss of absorbed energy during part of a cycle, but then a later retrieval of the energy, in such as way that the overall average power absorption is the same as if the controller had perfect knowledge of the WEC mass. However, this does assume a 100% efficient PTO system, where no parasitic energy dissipation occurs during the bi-directional power flow between the WEC and energy storage/grid. However, if PTO losses and/or constraints are considered, then the sensitivity towards accurate knowledge of the WEC mechanical impedance, inherent to the optimal controller, increases.

The relative comparison between the different controller performances, in Fig 10, is for the case of a scaled down version of a particular type of WEC. At full scale, or for different WEC types, the relative importance of various nonlinear hydrodynamic effects may differ. The results for the particular case presented, show the proposed ARHPC outperforming the other two controllers (when provided with exact future knowledge of the incident wave series). However, if the PI control parameters had also been adapted online, or if a different WEC type was tested, then different relative controller performances may have been observed. The NWT can be used as an evaluation tool, to assess the performance of different controller settings for different cases of WECs.

The NWT allowed the ARHPC to be tested and the performance appears promising. The tests suggest that the ARHPC could be performed in real-time for a real WEC, due to the quick linear optimisation in the RHPC algorithm and the relatively simple RLS algorithm for model parameter adaptation. The ARHPC parameter adaptation is seen to behave well, and resulted in a net positive effect for the control.

The results shown herein were for a simplified version of the real wave energy problem. For example, the WEC was a single body object, artificially restrained to heave motion, the mooring and PTO dynamics were ignored, and extensive verification and validation was not performed. To be a valuable evaluation tool for WEC performance, the NWT should match as close to reality as possible. Continual development of the NWT is therefore an active research focus, and future work endeavours to provide high fidelity simulations of all relevant physical effects of WEC operation, such as coupling PTO and mooring [50] models to the NWT simulation.

## VII. Conclusion

Enabling a EMC to adapt, based on measured data from the WEC operation, allows improved control performance. Due to uncertainty in system parameters, or parameter values changing with time, the EMC can use system identification techniques to build more accurate control models, that better describe the actual WEC dynamics in the current conditions.

This paper focussed on the performance of a linear control model in a nonlinear simulation. Better optimisation techniques are available for EMCs based on linear models, compared to those based on nonlinear models. The results here show the ability of a 'best fit' linear model in capturing relevant nonlinear effects, such as viscous damping.

A CFD NWT is shown to be a useful evaluation tool for adaptive controllers. the implementation of the adaptive control algorithm can be challenged, and debugged, in a simulation environment capable of capturing nonlinear hydrodynamic behaviour. The performance of the adaptive control can be easily assessed and compared against other results.

## VIII. Acknowledgement

This project is funded by Enterprise Ireland and is co-funded by the Irish Government and the European Union under Irelands EU Structural Funds Programme 2007- 2013 under grant EI/CF/2011/1320.

## References

[1] J. Scruggs, S. Lattanzio, A. Taflanidis, and I. Cassidy, "Optimal causal control of a wave energy converter in a random sea," *Applied Ocean Research*, vol. 42, pp. 1–15, 2013.

[2] J. Falnes, *Ocean Waves and Oscillating Systems*. Cambridge, UK: Cambridge University Press, 2002.

[3] U. Korde and J. Ringwood, *Hydrodynamic control of wave energy devices*. Cambridge University Press, New York, 2016.

[4] J. Hals, J. Falnes, and T. Moan, "A comparison of selected strategies for adaptive control of wave energy converters," *Journal of Offshore Mechanics and Arctic Engineering*, vol. 133, no. 3, 2011.

[5] G. Bacelli and J. V. Ringwood, "Numerical optimal control of wave energy converters," *IEEE Transactions on Sustainable Energy*, 2015.

[6] W. Cummins, "The impulse response function and ship motions," Tech. Rep., 1962.

[7] G. Giorgi and J. V. Ringwood, "Implementation of latching control in a numerical wave tank with regular waves," *Journal of Ocean Engineering and Marine Energy*, vol. 2, no. 2, pp. 211–226, 2016.

[8] J. Davidson, C. Windt, G. Giorgi, R. Genest, and J. Ringwood, "Evaluationg of energy maximising control systems for wave energy converters using OpenFOAM," in *OpenFOAM - Selected papers of the 11th Workshop*, Nbrega, J.M., Jasak, H. (Editors), Springer, 2018

[9] G. Giorgi, M. Penalba, and J. Ringwood, "Nonlinear hydrodynamic force relevance for different wave energy converter types," in *Proceedings of the $3^{rd}$ Asian Wave and Tidal Energy Conference (AWTEC)*, 2016.

[10] S. R. Nielsen, Q. Zhou, M. M. Kramer, B. Basu, and Z. Zhang, "Optimal control of nonlinear wave energy point converters," *Ocean Engineering*, vol. 72, pp. 176–187, 2013.

[11] G. Bacelli, R. Genest, and J. Ringwood, "Nonlinear control of a flap-type wave energy converter with a non-ideal power take-off system," *IFAC Annual Reviews in Control*, vol. 40, pp. 116–126, 2015.

[12] M. Richter, M. Magana, O. Sawodny, and T. Brekken, "Nonlinear model predictive control of a point absorber wave energy converter," *IEEE Transactions on Sustainable Energy*, vol. 4, no. 1, pp. 118–126, 2013.

[13] J. Davidson, S. Giorgi, and J. V. Ringwood, "Linear parametric hydrodynamic models for ocean wave energy converters identified from numerical wave tank experiments," *Ocean Engineering*, 2015.

[14] R. Genest and J. V. Ringwood, "Receding horizon pseudospectral control for energy maximization with application to wave energy devices," *IEEE Transactions on Control Systems Technology*, vol. 25, no. 1, 2017.

[15] J. Davidson and J. Ringwood, "Mathematical modelling of mooring systems for wave energy converters - a review," *Energies*, 2017.

[16] E. Anderlini, D. I. Forehand, P. Stansell, Q. Xiao, and M. Abusara, "Control of a point absorber using reinforcement learning," *IEEE Transactions on Sustainable Energy*, vol. 7, no. 4, pp. 1681–1690, 2016.

[17] J. V. Ringwood, J. Davidson, and S. Giorgi,"Identifying models using recorded data," in *Numerical Modeling of Wave Energy Converter: State-of-the-art techniques for single WEC and converter arrays*. Folley, M. (Editor), Elsevier, 2016.

[18] J. Davidson, S. Giorgi, and J. Ringwood, "Numerical wave tank identification of nonlinear discrete-time hydrodynamic models," in *1st Int. Conf. on Renewable Energies Offshore (Renew 2014), Lisbon*, 2014.

[19] S. Giorgi, J. Davidson, and J. V. Ringwood, "Identification of nonlinear excitation force kernals using numerical wave tank experiments," in *Proc. of the 11th European Wave and Tidal Energy Conference*, 2015.

[20] J. V. Ringwood, J. Davidson, and S. Giorgi, "Optimising numerical wave tanks tests for the parametric identification of wave energy device models," in *Proc. of the 34th Int. Conf. on Ocean, Offshore and Arctic Engineering (OMAE 2015)*, 2015.

[21] S. Giorgi, J. Davidson, and J. V. Ringwood, "Identification of wave energy device models from numerical wave tank datapart 2: Data-based model determination," *IEEE Trans. on Sustainable Energy*, 2016.

[22] K. J. Åström and B. Wittenmark, *Adaptive control*. Courier Corporation, 2013.

[23] K. J. Åström, "Theory and applications of adaptive controla survey," *Automatica*, vol. 19, no. 5, pp. 471–486, 1983.

[24] S. Behrens, J. Ward, and J. Davidson, "Adaptive vibration energy harvesting," in *The 14th International Symposium on: Smart Structures and Materials & Nondestructive Evaluation and Health Monitoring*. International Society for Optics and Photonics, 2007.

[25] G. Chatry, A. Clément, T. Gouraud *et al.*, "Self-adaptive control of a piston wave absorber," in *The Eighth International Offshore and Polar Engineering Conference*. International Society of Offshore and Polar Engineers, 1998.

[26] J. Davidson, S. Giorgi, and J. Ringwood, "Identification of wave energy device models from numerical wave tank data - Part 1: Numerical wave tank identification tests," *IEEE Trans. on Sustainable Energy*, 2016.

[27] G. Chatry, A. Clément, A. Sarmento *et al.*, "Simulation of a self-adaptively controlled owc in a nonlinear numerical wave tank," *International Journal of Offshore and Polar Engineering*, 2000.

[28] F. Fusco and J. V. Ringwood, "A simple and effective real-time controller for wave energy converters," *IEEE Transactions on sustainable energy*, vol. 4, no. 1, pp. 21–30, 2013.

[29] E. Tedeschi and M. Molinas, "Control strategy of wave energy converters optimized under power electronics rating constraints," in *3rd international Conference on Ocean Energy (ICOE10), Bilbao (SP)*, 2010.

[30] E. Tedeschi and M. Molinas, "Wave-to-wave buoys control for improved power extraction under electro-mechanical constraints," in *International Conference on Sustainable Energy Technologies (ICSET),*. IEEE, 2010.

[31] E. Tedeschi and M. Molinas, "Tunable control strategy for wave energy converters with limited power takeoff rating," *IEEE Transactions on Industrial Electronics*, vol. 59, no. 10, pp. 3838–3846, 2012.

[32] M. P. Schoen, J. Hals, and T. Moan, "Wave prediction and fuzzy logic control of wave energy converters in irregular waves," in *Control and Automation, 2008 16th Mediterranean Conference on*. IEEE, 2008.

[33] M. Jama, A. Assi, A. Wahyudie, and H. Noura, "Self-tunable fuzzy logic controller for the optimization of heaving wave energy converters," in *International Conference on Renewable Energy Research and Applications (ICRERA), 2012* .

[34] M. Jama, A. Wahyudie, A. Assi, and H. Noura, "An intelligent fuzzy logic controller for maximum power capture of point absorbers," *Energies*, vol. 7, no. 6, pp. 4033–4053, 2014.

[35] X. Xiao, X. Huang, and Q. Kang, "A hill-climbing-method-based maximum-power-point-tracking strategy for direct-drive wave energy converters," *IEEE Transactions on Industrial Electronics*, 2016.

[36] E. A. Amon, T. K. Brekken, and A. A. Schacher, "Maximum power point tracking for ocean wave energy conversion," *IEEE Transactions on Industry applications*, vol. 48, no. 3, pp. 1079–1086, 2012.

[37] U. A. Korde, R. D. Robinett, and D. G. Wilson, "Wave-by-wave control in irregular waves for a wave energy converter with approximate parameters," *Journal of Ocean Engineering and Marine Energy*, 2016.

[38] J. A. M. Cretel, G. Lightbody, G. P. Thomas, and A. W. Lewis, "Maximisation of energy capture by a wave-energy point absorber using model predictive control," in *Proc. $18^{th}$IFAC World Congress*, 2011.

[39] D. Huybrechs, "On the fourier extension of nonperiodic functions," *SIAM Journal on Numerical Analysis*, vol. 47, no. 6, 2010.

[40] B. Orel and A. Perne, "Computations with half-range chebyshev polynomials," *Journal of Computational and Applied Mathematics*, 2012.

[41] R. Genest and J. V. Ringwood, "A critical comparison of model-predictive and pseudospectral control for wave energy devices," *Journal of Ocean Engineering and Marine Energy*, pp. 1–15, 2016.

[42] M. H. Hayes, "9.4: Recursive least squares," *Statistical Digital Signal Processing and Modeling*, p. 541, 1996.

[43] F. Fusco and J. V. Ringwood, "Hierarchical robust control of oscillating wave energy converters with uncertain dynamics," *IEEE Transactions on Sustainable Energy*, vol. 5, no. 3, pp. 958–966, 2014.

[44] I. Kanellakopoulos, P. V. Kokotovic, and A. S. Morse, "Systematic design of adaptive controllers for feedback linearizable systems," *IEEE Transactions on Automatic control*, vol. 36, no. 11, pp. 1241–1253, 1991.

[45] J. Weber, "Wec technology readiness and performance matrix–finding the best research technology development trajectory," in *International Conference on Ocean Energy*, 2012.

[46] G. Giorgi, M. Penalba, and J. Ringwood, "Nonlinear Froude-Krylov force representations for heaving buoy wave energy converters," in *Proc. of the $3^{rd}$ Asian Wave and Tidal Energy Conference*, 2016.

[47] Y.-H. Yu and Y. Li, "Reynolds-averaged navier–stokes simulation of the heave performance of a two-body floating-point absorber wave energy system," *Computers & Fluids*, vol. 73, pp. 104–114, 2013.

[48] J. Davidson, M. Cathelain, L. Guillemet, T. Le Huec, and J. Ringwood, "Implementation of an openfoam numerical wave tank for wave energy experiments," in *Proceedings of the 11th European Wave and Tidal Energy Conference*, 2015.

[49] G. Giorgi and J. V. Ringwood, "Implementation of latching control in a numerical wave tank with regular waves," *Journal of Ocean Engineering and Marine Energy, in press*, 2016.

[50] J. Palm, C. Eskilsson, G. Moura Paredes, and L. Bergdahl, "CFD simulation of a moored floating wave energy converter," in *Proc. 10th European Wave and Tidal Energy Conference*, 2013.

[51] N. G. Jacobsen, D. R. Fuhrman, and J. Fredsøe, "A wave generation toolbox for the open-source cfd library: Openfoam®," *International Journal for Numerical Methods in Fluids*, vol. 70, pp. 1073–1088, 2012.

[52] P. Schmitt and B. Elsäßer, "The application of Froude scaling to model tests of Oscillating Wave Surge Converters", *Ocean Engineering*, 2017

[53] J. Falnes, *Ocean Waves and Oscillating Systems : linear interactions including wave-energy extraction*. Cambridge Universtity Press, 2002.

[54] C. Eskilsson, J. Palm and L. Bergdahl,"On numerical uncertainty of VOF-RANS simulations of wave energy converters through V&V technique" in *Proceedings of the 12th European Wave and Tidal Energy Conference*, 2017.

[55] C. Windt, J. Davidson, P. Schmitt, and J.V. Ringwood,"Assessment of Numerical Wave Makers" in *Proceedings of the 12th European Wave and Tidal Energy Conference*, 2017.

[56] A. Merigaud and J. Ringwood, "Optimal trajectories, nonlinear models and constraints in wave energy device control," in *International Federation of Automatic Control (IFAC)*, 2017.